Adsorption of arsenic using low-cost adsorbents: Guava leaf biomass, mango bark and bagasse

Devendra Mohan[1*], Markandeya[1], S. Dey[1], S.B. Dwivedi[1] and S.P. Shukla[2]

[1]Department of Civil Engineering, Indian Institute of Technology (BHU) Varanasi-221005, India

[2]Department of Civil Engineering, Institute of Engineering and Technology, Lucknow-226021, India

[*]Author for correspondence: +91-9451173756;

E-mail IDs: devmohan9@gmail.com (Devendra Mohan)

mktiwariiet@gmail.com (Markandeya)

subha11ashi@gmail.com (S. Dey)

dwivedi12@iitbhu.ac.in (S.B. Dwivedi)

sps.iet@gmail.com (S.P. Shukla)

Abstract

Adsorbents prepared from inexpensive material of guava leaf biomass, mango bark and bagasse have been investigated for the possibility to be used as adsorbents for the removal of As(III) from the aqueous solution. The effects of pH, contact time, initial As(III) concentration and adsorbent dosage on the adsorption of As(III) have been investigated using batch experiments. Adsorption process was also verified with Langmuir, Freundlich, Temkin and Redlich-Peterson models. Langmuir isotherm fitted best in experimental data. Application of Langmuir isotherm to the system yielded maximum capacity of 1.35 $mg.g^{-1}$, 1.25 $mg.g^{-1}$ and 1.05 $mg.g^{-1}$ for bagasse, mango bark and guava leaf biomass, respectively in the range of As(III) concentration as 10-140 $mg.L^{-1}$. The dimensionless equilibrium parameter, R_L, signifies a favorable adsorption of As(III) on all of adsorbents and was observed to be in the range of 0.029-0.294, 0.021-0.235 and 0.021-

0.234, for bagasse, mango bark and guava leaf biomass, respectively ($0<R_L<1$). The adsorption process was observed to follow pseudo-second-order kinetic model.

Keywords: Adsorption; Isotherms; Kinetics; Low-cost adsorbents; Arsenite ion-As(III)

1. Introduction

During the past few decades, arsenic has gradually been identified as one of the most toxic substances in water and wastewater around the world, which weakens the immune system and threatens the human health (Shukla et al., 2015). Arsenic content in groundwater varies with the geographical location, geological conditions and role of anthropogenic activities. Human activities resulting in appearance of arsenic in ground water are mainly the use of arsenical pesticides, fertilizers, desiccants, preservatives, dust from the burning of fossil fuels and disposal of industrial and animal wastes, etc. (Choong et al., 2007; Shevade and Ford, 2004). Approximately, 97% of the arsenic produced enters through the end-product manufactured in the form of white As(III) and the remaining 3% as semi-metal employed metallurgical additives, especially to lead and copper to produce their alloys (U.S. Department of the Interior Bureau of Mines). Inorganic arsenic of geogenic (natural) origin is also found in groundwater in certain parts of the world, which is supported to arise from volcanic action followed by low-temperature volatization (Mandal and Suzuki, 2002). Arsenic may also be naturally present in all rocks and sediments, forming aquifers tapped for drinking (USEPA, 2007). It has been reported that areas affected by geothermal, mining and industrial activities may suffer from presence of large range of arsenic varying from 0.5 to 5000 $\mu g.L^{-1}$ (Mohan and Charles, 2007). There are 21 arsenic affected countries worldwide and out of these, Bangladesh (concentration greater than 0.2 $mg.L^{-1}$) and the state of West Bengal in India (highest 470 $mg.L^{-1}$) are at high health risk due to arsenic contaminated groundwater (Rahmanet al., 2002).

In groundwater, arsenic may combine with oxygen and form inorganic pentavalent arsenate, As(V) and trivalent arsenite, As(III) depending on the pH and redox conditions (Natale et al., 2008). As(III) is more stable than As(V) due to the electronic configuration and also, relatively more toxic because it can bind with higher affinity to vicinal sulfhydryl groups, that have the capability to react with a variety of proteins and thus, inhibit their activity (Peggy, 2006). It has been established that exposure to arsenic may lead to both, acute as well as chronic toxicity, resulting in many adverse impacts on human health like hematological, hepatic, renal, dermal, neurological, developmental, reproductive, immunologic, genotoxic, mutagenic, carcinogenic, hematological/hepatic including other biological effects (Mandal and Suzuki, 2002). Certain severe diseases have been faced by humans due to consumption of arsenic contaminated water and these include cancers of liver, lungs, skin, kidney and bladder; pigmentation changes, hyperkeratosis, neurological and gastrointestinal disorders, muscular weakness, bone marrow, cardiovascular problems etc. (Mandal and Suzuki, 2002). Therefore, arsenic contamination of groundwater has been taken worldwide as an urgent environmental issue that requires serious attention immediately. To overcome this situation, earlier provisional guidelines of WHO and USEPA has been brought down from 50 to 10 ppb as drinking water quality standard (WHO, 2001; USEPA Federal Register, 2001).

Several technologies are available now for the treatment of arsenic contaminated water (Mohan and Charles, 2007), amongst which the most common techniques are oxidation/ precipitation/ filtration (Leupin and Hug, 2005), coagulation/ electro-coagulation/ co-precipitation (Wickramasingheet al., 2004), ion exchange resin (Kim and Benjamin, 2004), membrane techniques like ultra/ nano-filtration/ reverse osmosis/ electrolysis (Weng et al., 2005) etc.

69 The conventional practice of arsenic removal (at large scale) is to first oxidize As(III) into
70 As(V), employing either chemical or biological routes and then, using any media like iron/
71 manganese or alumina for adsorption. Though these chemical methods are simple, large amounts
72 of toxic sludge are produced that requires further treatment before the ultimate disposal. Ion-
73 exchange resins require high cost, high-tech operation and maintenance and regeneration
74 (feasible partially) and creates sludge disposal problems. Membrane based techniques also need
75 high initial as well as operation and maintenance cost along with rejection of water in sizeable
76 quantities. Other limitation associated with most of the conventional treatment methods is
77 efficiency of the treatment, i.e., they are not much effective at lower concentrations and even
78 after treatment, the residual concentrations may remain higher than the permissible limit with
79 respect to the drinking water quality standards i.e. 10 $\mu g.L^{-1}$ (Jain and Singh, 2012).
80 The process of adsorption involves a solid phase (adsorbent) and a liquid phase containing
81 dissolved species to be adsorbed. Agricultural waste-materials are usually composed of lignin,
82 cellulose, lipids, proteins, polysaccharides, hydrocarbons, ash and many other compounds as a
83 variety of functional groups (Sud et al., 2008). These groups present on the solid materials cause
84 affinity to adsorb the ionic species (adsorbate) present in solution. This phenomenon depends
85 upon bonding linkages between species of the adsorbate in solution and molecules of the solid
86 materials. Any solid material may be employed as adsorbent, if it has sufficient affinity to adsorb
87 the target species. Local and abundant availability, low cost of preparation and high capacity to
88 adsorb make an effective adsorbent (Tiwari et al., 2015). Bonding linkages between the metal
89 species and molecules of adsorbent depend upon a complex mechanism, through which metal
90 species are diffused to the adsorbent surface and its inner pores. Many mechanisms have been
91 proposed to explain the removal at the adsorbent surface and pores involving chemisorption,

92 complexation, ion exchange, chelation, physical forces, entrapment in inter and intra-fibrillar
93 capillaries etc. (Qaiser et al., 2007).
94 Proper understanding of the adsorption mechanism, rate of adsorption, maximum adsorption
95 capacity and suitable pH range, contact time to reach equilibrium, initial adsorbate concentration
96 and dosage of adsorbent are essential parameters needed for the system design. To understand
97 the kinetics and equilibrium isotherms, batch study has been undertaken to investigate various
98 related parameters fitting into appropriate models. Finally, these parameters were correlated to
99 understand the adsorption mechanism for more toxic form, i.e., As(III), from the water on the
100 surface of biosorbents prepared from agricultural waste like bagasse, mango bark and biomass of
101 guava leaf.
102 As an alternative or a part of tertiary water treatment, adsorption has long been recognized as an
103 effective technique and it is being used, specifically more commonly in the developing world to
104 treat the arsenic contaminated water up to the desired level of efficiency. Researchers had been
105 putting effort to investigate new adsorbents that are easily and locally available as well as have
106 low-cost of preparation, operation and handling (Mohanet al., 2007; Wang and Chen, 2009).
107 Now-a-days, various solid wastes generated as byproducts of industry/ agriculture is under
108 investigation to assess the adsorption potential for arsenite ions present in water. With the
109 objective of developing a novel and low-cost adsorbents to remove As(III) from water, guava
110 leaf biomass, mango bark and bagasse have been employed as inexpensive agriculture waste and
111 their adsorption capacities have been evaluated for As(III) removal under equilibrium and
112 dynamic experimental conditions.
113 **2. Materials and Methods**
114 **2.1 Adsorbents**

115 The guava leaf biomass, mango bark and bagasse were collected within the campus of Indian
116 Institute of Technology (BHU) Varanasi India. Subsequently, all these were cleaned with
117 distilled water and then, air dried in hot air oven at a temperature of 60°C for 24 hr. Afterwards,
118 these were crushed and passed through British Standard sieves in the range of 0.425 mm to 1.180
119 mm. The adsorbents were activated by treating with acids, which increase effectiveness of
120 adsorption by enhancement in active sites per unit surface area. This also provides better ion
121 exchange properties due to formation of new functional groups (Babu and Gupta, 2008;
122 Montagnaro and Santoro, 2009; Wang et al., 2005). Several acidic treatments were experimented
123 to improve the adsorption properties of the sorbents. Finally, HCl (0.1N) was used to activate the
124 biomass derived from guava leaf, mango bark and bagasse. Activation was performed by treating
125 1 g of the residue retained on screens with 100 mL of acidic solution for 6 hr at 55°C under
126 continuous stirring and subsequently, followed by filtration and oven drying at 55°C for 24 hr.
127 The oven dried sample was washed with distilled water to remove residual acid from the surface
128 until the runoff was visibly clear. Then, this sample was dried again at 110°C for 12 hr and after
129 this, kept in capped bottles.

130 **2.2 Adsorbate**

131 All chemicals used were of analytical grades. A stock As(III) solution (1 mL = 1000 µg As) was
132 prepared by dissolving 0.1320 g of As_2O_3 in a mixture of 50 mL of reagent grade water and 1
133 mL conc. NH_4OH. It was heated gently to dissolve completely, cooled and acidified with 2 mL
134 conc. HNO_3. Then, it was diluted to 100 mL with reagent grade water.

135

2.3 Batch adsorption studies

Batch adsorption studies were conducted in 250 mL erlenmeyer flask by agitating a pre-weighted amount of the adsorbent with 100 mL of aqueous As(III) solution for a fixed time (100 min) period at constant temperature (25 ± 1°C) on a water bath shaker at 100 rpm. The pH was maintained (ranging from 2 to 8) at a desired value ± 0.1 using 0.01 to 0.05 N H_2SO_4 and NaOH at an interval of every 1 to 2 hr or as and when needed. The supernatants were passed through a filter paper number 42 (Whatman). Adsorption isotherm study was also carried out with varying concentration of As(III) from 10 to 140 $mg.L^{-1}$ while maintaining the adsorbent dosage of 8 g (bagasse and mango bark) and 9 g (guava leaf), placed in the solution taking equilibrium time of 100 min. The effects of variation in parameters like pH, contact time and initial concentration were studied keeping constant adsorbent dosage of 8 g (bagasse and mango bark) and 9 g (guava leaf) in contact with As(III) solution, having concentration of 100 $mg.L^{-1}$.

Effect of adsorbent dosage was studied at 100 $mg.L^{-1}$ of As(III) concentration with varying adsorbent dosage from 1 to 12 g in the solution. The concentration of free As(III) ion in the filtrate was determined using Arsenator (make Wagtech, U.K.). The values were also verified randomly specified in the procedure 3500-A, in the standard method 2012 using atomic absorption spectrophotometer (make Shimadzu, model AA 6800) with continuum background correction. For the atomic absorption spectrophotometer, all measurements were based on integrated absorbance and performed at 193.7 nm by using a hollow cathode lamp. The experiments were performed in triplicate and the average values were considered.

Amount of the adsorbed As(III) was calculated by finding difference of the initial and residual amounts of As(III) in the solution divided by mass of the adsorbent used as shown in mass balance equation (1). Percentage removal of As(III) was determined using equation (2).

$$q = \frac{(C_o - C_e) \times V}{m_s} \quad (1)$$

$$R\ (\%) = \frac{(C_o - C_e)}{C_o} \times 100 \quad (2)$$

Where, q is the amount of As(III) adsorbed by the adsorbent ($mg.g^{-1}$), C_o and C_e are the initial and equilibrium concentrations of As(III) in the solution ($mg.L^{-1}$), V is the total volume of the sample (100 mL), m_s is the mass of adsorbent used for adsorption (g) and R is the percentage of As(III) removal efficiency of the corresponding adsorbent.

3. Results and Discussion

Adsorption percentage of As(III) removal on activated powder of bagasse, mango bark and guava leaf were observed at initial concentration of 10 $mg.L^{-1}$ under optimized pH range and adsorbent dosage. Removal was reported as 95.2%, 97.2% and 94.4% for bagasse, mango bark and guava leaf, respectively. Maximum adsorption capacity at 140 $mg.L^{-1}$ of As(III) was found to be 1.191 $mg.g^{-1}$, 1.155 $mg.g^{-1}$ and 0.968 $mg.g^{-1}$, for bagasse, mango bark and guava leaf, respectively. Various researchers (Singh and Pant, 2004; Vaishya and Gupta, 2002) have made comparison of the adsorbent capacities for treatment of drinking water, groundwater and wastewater. This comparison with the adsorbent capacity and initial concentration of As(III) in case of previously studied adsorbents revealed that the adsorbents prepared from bagasse, mango bark and guava leaf biomass can be effectively used as alternate economical materials for removal of As(III) from wastewater.

3.1 Batch studies

3.1.1 Effect of pH

Studies indicate that As(III) ionic species is pH dependent and it is stable at pH < 9 in the form of neutral H_3AsO_3, pH 9 to 12 as $H_2AsO_3^-$, pH 12 to 13 as $HAsO_3^{2-}$ and pH > 13 as AsO_3^{3-} respectively (Jeong et al., 2007). Dissociation mechanism of arsenite species is reported by

182 Tamas et al. (2014) in terms of its acid dissociation constant (pK_a). The larger the value of pK_a,
183 lower the probability to dissociate at any pH and so, it is relatively difficult to dissociate H_2AsO_3
184 and $H_2AsO_3^-$. Equilibrium data of the experiments in this study have also confirmed the species
185 H_3AsO_3 as an active arsenite species by giving effective adsorption of As(III) in the pH range of
186 2 to 8 at surface of all the three adsorbents.

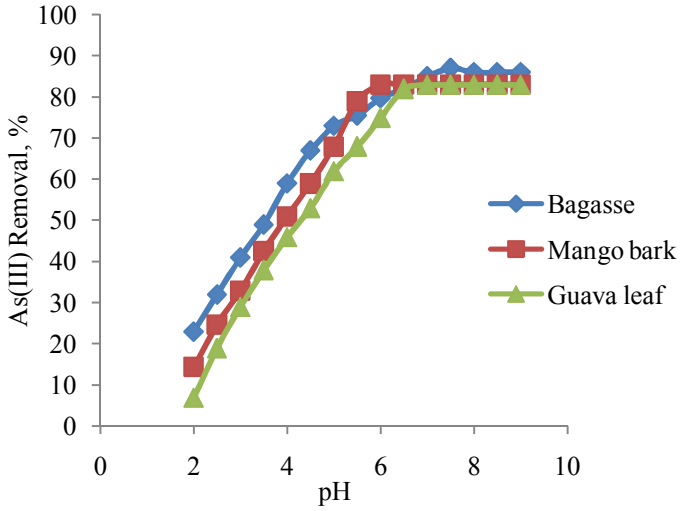

187

188 Figure 1: Effect of pH on As(III) adsorption

189 Increase in As(III) removal was observed from 23 to 73% (bagasse), 7 to 62% (mango bark) and
190 14 to 68% (guava leaf biomass) at increasing rate when pH was raised from 2 to 6 and only
191 slight removal could take place in pH range of 6 to 7 (Fig. 1). The maximum removal of 87%
192 was observed at pH 7.5 for bagasse, 84% at pH 6.5 for mango bark and 83% at pH 6 for guava
193 leaf biomass. Further increase in pH beyond these values showed slight reduction in As(III)
194 removal. It was observed that pH 7.5, 6.5 and 6.0 can be considered as optimum pH value for
195 As(III) removal by adsorption on the adsorbent surfaces of bagasse, mango bark and guava leaf
196 biomass, respectively. The pH dependence on adsorption can be understood as affinity of each
197 arsenic species to the adsorbent is different and therefore, the degree of adsorption of As(III) on
198 the adsorbent surfaces of bagasse, mango bark and guava leafs varied with the arsenic species

and thus, with pH value of the solution. Salman et al. (2011) reported that the adsorption was more effective on acid-treated adsorbents and therefore, adsorbents of guava leaf biomass, bagasse and mango bark were activated using 0.1N HCl at 55°C. At this temperature, activated adsorbents generally develop acidic surface oxides in the pH range of 6 to 8, while the surfaces of adsorbents become positively charged to adsorb more arsenite ions.

3.1.2 Effect of contact time

Results presented in Fig. 2 reveal the effect of contact time at optimum pH 7.5, 6.5 and 6.0 can be considered as value for As(III) removal by adsorption on bagasse, mango bark and guava leaf biomass respectively. Three stages of adsorption can be observed in each case and these indicate high influence of contact time on removal of As(III) by adsorption. First stage of As(III) uptake at adsorbent surfaces occurred at high rate during 0 to 90 min and removal up to 83% for bagasse, 82% for mango bark and 81% for guava leaf biomass could be achieved. On further increase in contact time, almost negligible enhancement in adsorption was observed. Therefore from Fig. 2, it can be concluded that the contact time of 100 min may be considered as an equilibrium time for adsorption of As(III) for all adsorbents while carrying out batch studies in the present case. Adsorption sites with formation of bi-dentate complexes are provided within very short duration and beyond this stage, no adsorbent site remains for further adsorption because saturation was achieved on the adsorbent surfaces (Carabanteet al., 2009).

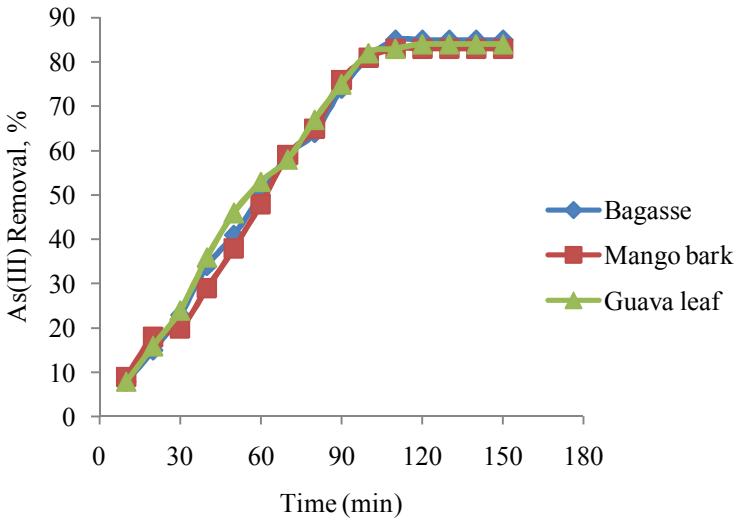

Figure 2: Effect of contact time on As(III) adsorption

3.1.3 Effect of initial concentration

Influence of initial concentration of As(III) on removal by adsorption was studied at concentration varying from 10 to 140 mg.L^{-1}, while maintaining the adsorbent dosage 8.0 g (bagasse and mango bark) and 9 g (guava leaf biomass) respectively in solution at optimized pH and contact time. Fig. 3 shows the effect of initial concentration of As(III) on percentage removal and adsorption capacity. Decrease in percentage removal was observed from 95.4% to 68.0% for bagasse, 97.2% to 68.0% for mango bark and 96.4% to 62.2% for guava leaf biomass, when concentration of solute was increased from 10 to 140 mg.L^{-1} at fixed contact time and pH. The results indicated that a very small reduction in removal occurred, when concentrations varied from 10 to 70 mg.L^{-1}; but afterwards, increase in concentration led to rapid reduction in As(III) removal. The drop in percentage As(III) removal is due to increase in the number of As(III) ions for fixed number of adsorbent sites. It was further observed that surface of mango bark showed the maximum value of removal as compared to guava leaf biomass and bagasse in between 10 to 60 mg.L^{-1} of As(III) concentration, but the results also indicated that this affinity did not remain so at higher As(III) concentration. Katsoyiannis and Zouboulis (2004) have

reported that during physicochemical iron oxidation, arsenate removal was about 80% for relatively lower initial arsenic concentrations (20–50 μg.L^{-1}) and it decreased to about 60%, when initial arsenic concentration was increased further to 188 mg.L^{-1}.

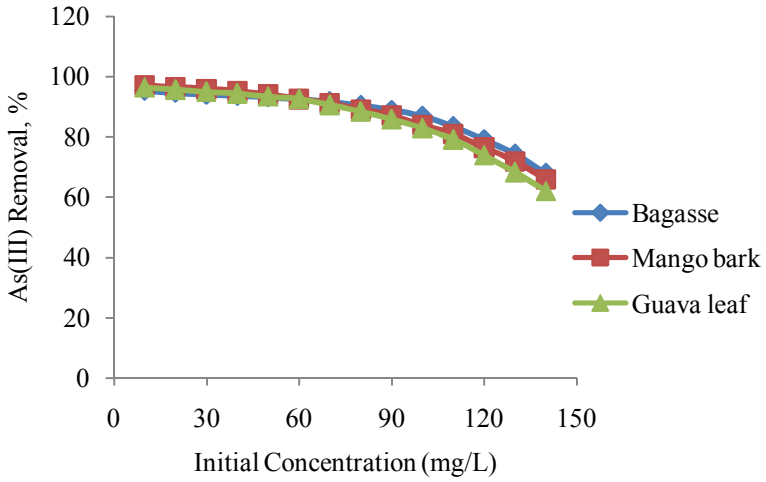

Figure 3: Effect of initial concentration on As(III) adsorption

Bagasse showed higher affinity as compared to mango bark and guavas leaf at higher arsenic concentration. However, the same adsorption percentage was observed on each adsorbent at 60 mg.L^{-1} of arsenic concentration and this indicated towards equal affinity to adsorb arsenite species at this concentration (Fig. 3).

Possibility of interference of previously adsorbed species can also not be ruled out and it may reduce As(III) adsorption and desorption from adsorbent molecules, which results ultimately into decreased adsorption capacity. Value of optimum percentage removal at 60 mg.L^{-1} was observed as 89.76% for bagasse, 88.34% for mango bark and 85.84% for guava leaf biomass respectively; while those for optimum adsorption capacity were 0.974 mg.g^{-1} for bagasse, 0.937 mg.g^{-1} for mango bark and 0.859 mg.g^{-1} for guava leaf biomass.

3.1.4 Effect of adsorbent dosage

Results of the batch studies conducted for determination of adsorbent dosage at initial concentration of As(III) as 60 $mg.L^{-1}$ with varying dosage of 4 to 12 g under optimized environmental conditions are presented in Fig. 4. Increase in As(III) percentage removal was observed with increase in amount of adsorbent dosage. The percentage removal increased from 55% to 87% (bagasse), 50% to 84% (mango bark) and 46% to 83% (guava leaf biomass). Higher percentage removal of As(III) was due to availability of more active adsorbent sites for adsorption at higher adsorbent dosage. But, capacity to adsorb As(III) was not same for each adsorbent dosage. Explanation in terms of adsorption sites can be given using a ratio factor of active adsorbent sites per unit mass of the adsorbents. This factor can also be correlated with apparent energy of sorption defined by Langmuir and the values lower than unity indicate toward decrease in the adsorption capacity.

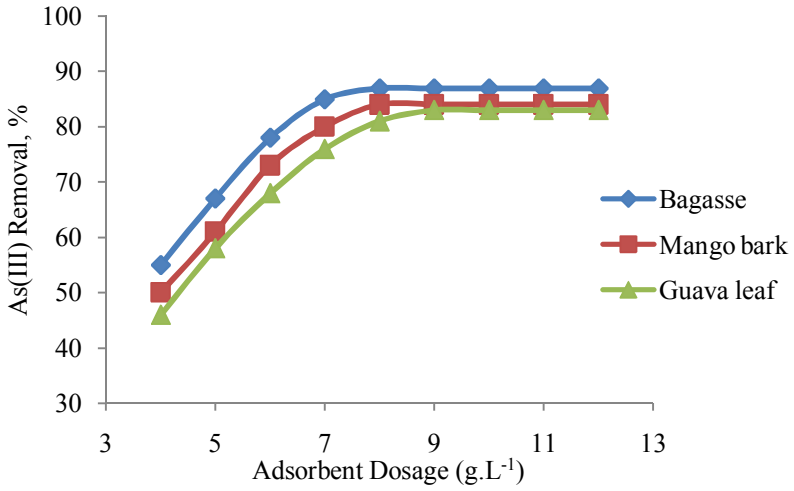

Figure 4: Effect of adsorbent dosage on As(III) adsorption

Results shown in Fig. 4 indicate that increased rate of removal of As(III) occurred only at certain adsorbent dosage and on further increase in dosage, adsorption rate remains the same due to the fact that all available adsorbate at particular concentration become attached at the active sites

present in the solid adsorbent and therefore, further addition of adsorbent did not cause any significant enhancement in adsorption. Shipley et al. (2009) have studied adsorption of arsenic on magnetite nano-particles and observed that as the dosage of adsorbent increase from 0.05 $g.L^{-1}$ to 0.2 $g.L^{-1}$, removal of As(III) also went up from 38.2 $\mu g.L^{-1}$ to 77.6 $\mu g.L^{-1}$.

Significant adsorption of As(III) on the adsorbent surfaces of bagasse and mango bark was observed in the range of adsorbent dosage of 4 to 8 g, and 4 to 9 g for guava leaf biomass respectively (Fig. 4). Further addition of adsorbent dosage remained ineffective for adsorption. Therefore, for the batch study, 8 g of dosage was considered as saturation dosage for bagasse and mango bark, and 9 g for guava leaf biomass respectively as shown in Table 1.

3.2 Adsorption isotherms

Mass of As(III) adsorbed per unit mass of the adsorbents is defined as adsorption capacity of the adsorbent. Nature of adsorption can be explained by relating the adsorption capacity to equilibrium concentration of the adsorbate remaining in the solution using various isotherms (Markandeyaet al., 2015; Shukla et al., 2017). Most common adsorption isotherms are Langmuir (1918), Freundlich (1906), Temkin and Pyzhev (1940), Redlich-Peterson (1950) etc. In present study, isotherms were plotted for each of the adsorbents using the experimental data (Fig. 5). Equilibrium data of these isotherms have been analyzed using the theories proposed by Freundlich, Langmuir, Temkin and Redlich-Peterson. Corresponding parameters calculated using these models are presented in Table 1.

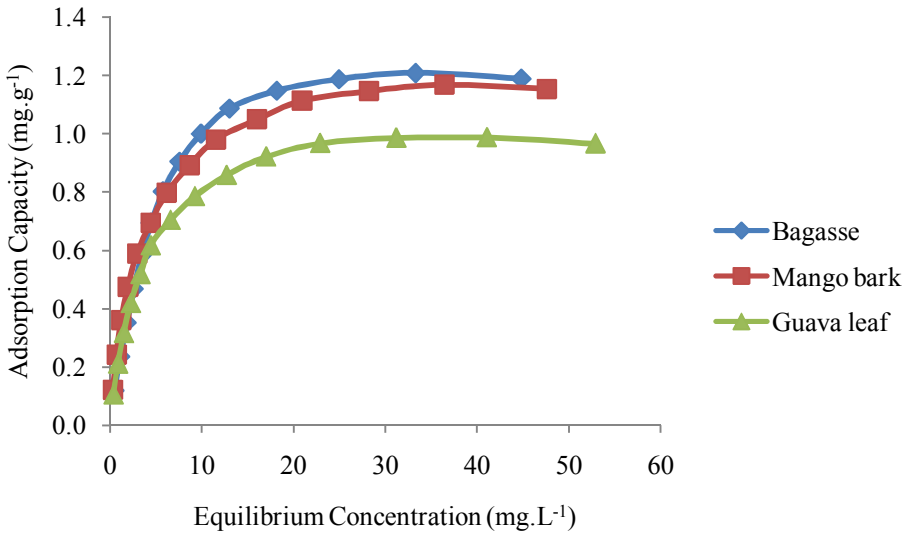

Figure 5: Adsorption isotherms on As(III) adsorption

3.2.1 Freundlich isotherm

Freundlich (1908) derived an empirical equation to describe non-ideal multilayer sorption on heterogeneous surface energy systems. Isotherms were defined by him over a limited range of concentration and these can be shown by equation (3). Linear form of Freundlich expression is presented in equation (4).

$$q_e = K_f C_e^{1/n} \quad (3)$$

$$\mathrm{Ln}\, q_e = \mathrm{Ln}\, K_f + \frac{1}{n} \mathrm{Ln}\, C_e \quad (4)$$

Where q_e is solid phase sorbent concentration at equilibrium ($mg.g^{-1}$), C_e is aqueous phase sorbent concentration at equilibrium ($mg.L^{-1}$), n is Freundlich constant that represents the parameter characterizing Quasi-Gaussian energetic heterogeneity of the adsorption surface (Markandeya et al., 2017a,b,c) and K_f is another Freundlich constant, indicative of the relative adsorption capacities of the adsorbents ($L.g^{-1}$).

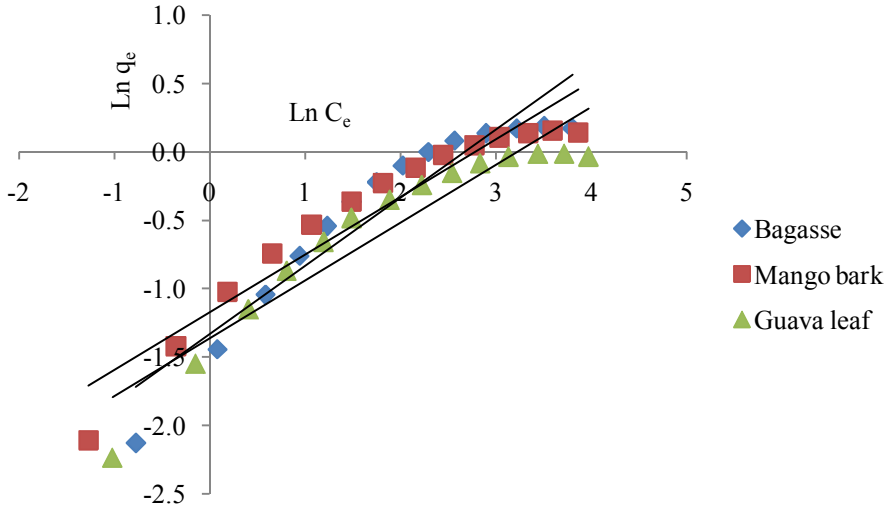

Figure 6: Freundlich isotherms on As(III) adsorption

Freundlich isotherm was tested to understand the adsorption intensity of As(III) on the adsorbent surfaces of bagasse, mango bark and guava leaf biomass. The experimental data were plotted logarithmically (Fig. 6), applying the linear Freundlich isotherm equation (4).

The linear Freundlich isotherm constants for As(III) adsorption are presented in Table 2.

3.2.2 Langmuir isotherm

Langmuir described adsorption as a result of formation of an ionic or covalent bond between adsorbent and adsorbate molecules and defined fractional coverage (θ) in the form equation (5).

$$\theta = \frac{q_e}{q_m} = \frac{b\,C_e}{1 + b\,C_e} \qquad (5)$$

Where, 'b' is a parameter for apparent energy of sorption, defined as, $b = (k_a/k_d)$, 'k_a' and 'k_d' are constants for adsorption and desorption respectively. 'q_m' is the maximum quantity of As(III) required to form a single monolayer on unit mass of adsorbent, q_e is sorbate concentration on solid phase at equilibrium ($mg.g^{-1}$) and C_e is aqueous phase sorbate concentration at equilibrium ($mg.L^{-1}$). Linearization of equation (5) yields equation (6) and can be expressed as Langmuir

isotherm, from which values of the constant 'b' and 'q_m' can be determined from the slope and intercept by plotting C_e/q_e vs C_e (Markandeya et al., 2017d; Weber et al., 1972).

$$\frac{C_e}{q_e} = \frac{1}{b\,q_m} + \frac{1}{q_m}(C_e) \quad (6)$$

Langmuir isotherm has been considered to estimate the maximum adsorption capacity corresponding to the monolayer coverage on the adsorbents surfaces. Plots of specific sorption (C_e/q_e) against C_e for these adsorbents are shown in Fig. 7 and the isotherm parameters, q_m, b and R^2 are presented in Table 1. The sorption capacity, q_m has higher value for bagasse (1.346 $mg.g^{-1}$) in comparison to the values for mango bark (1.249 $mg.g^{-1}$) and guava leaf biomass (1.052 $mg.g^{-1}$), respectively. From the results, it can be understood that bagasse has more capacity to adsorb As(III) than that of mango bark and guava leaf biomass. The adsorption coefficient, b for As(III) on guava leaf biomass (0.327 $L.mg^{-1}$) was greater than that of mango leaf (0.326 $L.mg^{-1}$) and bagasse (0.240 $L.mg^{-1}$) (Table 1). It indicated that, the effectiveness of As(III) adsorption on the adsorbents surface was bagasse > mango bark > guava leaf biomass. The value of R^2 for As(III) adsorption on surface of mango bark (0.999) was greater than guava leaf biomass (0.998) and bagasse (0.996) (Fig. 7). It leads to conclusion that adsorption on guava leaf biomass fits better than that on bagasse and mango bark.

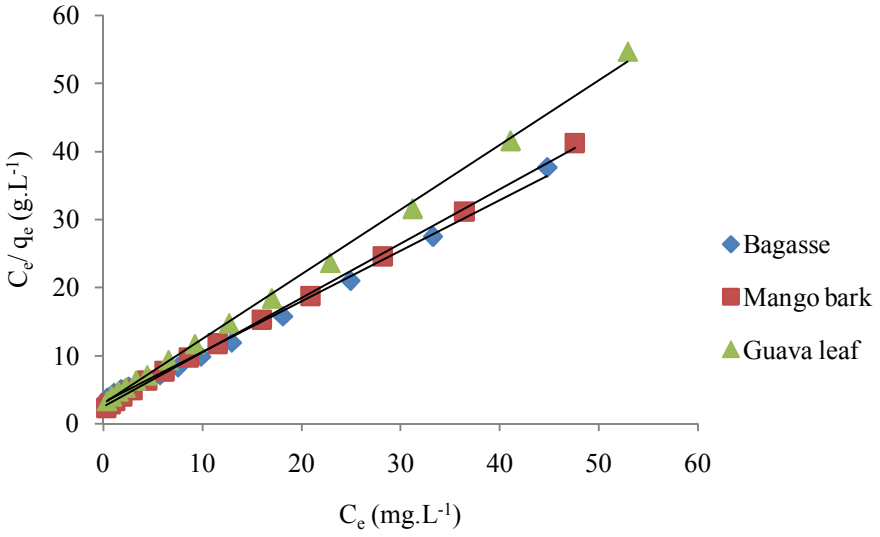

Figure 7: Langmuir isotherms on As(III) adsorption

Furthermore, appropriateness of As(III) adsorption on the adsorbents was tested using features of Langmuir isotherm, expressed in terms of a non-dimensional constant, called separation factor R_L and it is defined by equation (7) (Markandeyaet al., 2017).

$$R_L = \frac{1}{1 + b\,C_O} \qquad (7)$$

Where, 'C_o' (mg.L^{-1}) is the initial concentration of arsenite solution and 'b' (L.mg^{-1}) is Langmuir isotherm constant. Value of R_L should be between 0 and 1 for favorable adsorption, R_L>1 represents unfavorable conditions. R_L = 1 indicate towards linear adsorption, while adsorption process is irreversible, if R_L = 0. R_L value for adsorption of arsenic on surface of the adsorbents was found to be in the range of 0.029 to 0.294 (bagasse), 0.021 to 0.235 (mango bark) and 0.021 to 0.234 (guava leaf biomass) under different conditions. Values of the separation parameter for all adsorbents being less than unity indicate that all adsorbents could provide favorable conditions (to different degrees) for adsorption of As(III). The smaller R_L value indicates a highly favorable adsorption and R_L values of guava leaf biomass > mango bark > bagasse.

3.2.3 Temkin isotherm

Temkin isotherm is represented by equation (8) and on linearization; it can be given by equation (9).

$$q_e = \frac{RT}{B_t} Ln(K_T C_e) \quad (8)$$

$$q_e = B_t \ln K_T + B_t \ln C_e \quad (9)$$

Where, T is absolute temperature (K), R is the universal gas constant (8.314 $J.mol^{-1}.K^{-1}$), K_T is the equilibrium binding constant ($L.mg^{-1}$) and B_t is Temkin constant related to the heat of adsorption ($kJ.mol^{-1}$). Temkin isotherm was also plotted to understand adsorption phenomenon of these adsorbents. Temkin isotherm plots for these three adsorbents are presented in Fig. 8 and the isotherm parameters in Table 1. Values of Temkin adsorption potential, K_T, for mango bark, guava leaf biomass and bagasse were found to be 4.834 $L.mg^{-1}$, 4.262 $L.mg^{-1}$ and 2.697 $L.mg^{-1}$ respectively. It indicates a lower adsorbent-As(III) potential of bagasse and highest for mango bark among the adsorbents. Temkin constant, B_t, related to heat of sorption for As(III) adsorption on the adsorbents and higher value is reported for bagasse (0.278 $kJ.mole^{-1}$) rather than mango bark (0.230 $kJ.mole^{-1}$) and guava leaf biomass (0.201 $kJ.mole^{-1}$). It has been reported (Ho, Porter, McKay, 2002) that the typical range of bonding energy for ion-exchange mechanism is 8 to 16 $kJ.mole^{-1}$.

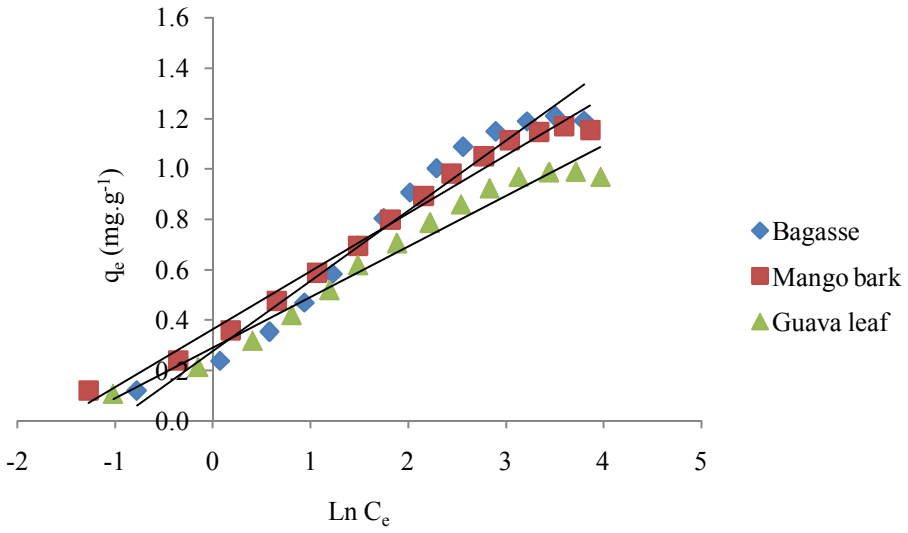

Figure 8: Temkin isotherms on As(III) adsorption

3.2.4 Redlich-Peterson isotherm

Redlich and Peterson suggested an isotherm equation (10) having three adsorption parameters in 1959, unanimously called Redlich-Peterson (R-P) isotherm. This equation amends inaccuracies of two parameter Langmuir and Freundlich isotherms equation in adsorption systems and can be written in equation (10) and on further linearization in equation (11).

$$q_e = \frac{(q_m\ b_{RP})C_e}{1 + b_{RP}\ C_e^{\alpha_{RP}}} = \frac{(K_{RP})C_e}{1 + b_{RP}\ C_e^{\alpha_{RP}}} \qquad (10)$$

$$\frac{C_e}{q_e} = \frac{1}{K_{RP}} + \frac{b_{RP}}{K_{RP}} C_e^{\alpha_{RP}} \qquad (11)$$

Where, K_{RP} ($L.g^{-1}$), b_{RP}($L.m^{-1}.mol^{-1}$) and α_{RP} are Redlich-Peterson constants and q_m is the maximum quantity of adsorbate required to form a single monolayer on unit mass of adsorbent. Redlich-Peterson isotherm constants can be predicted from the plot between C_e/q_e vs $C_e^{\alpha_{RP}}$. It has been experimentally proved that when $\alpha_{RP} = 1$, Redlich-Peterson isotherm reduces into Langmuir isotherm, similarly when intercept of equation (11) is closest to zero, it reduces to Freundlich isotherm (Feng-Chin et al., 2010).

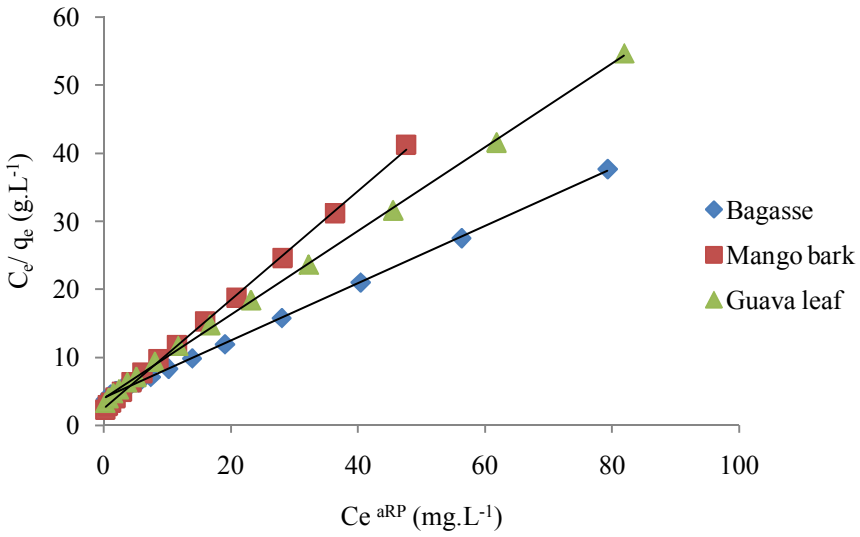

Figure 9: Redlich-Peterson isotherms on As(III) adsorption

Linearized form of Redlich-Peterson isotherm equation contains three unknown parameters K_{RP}, b_{RP} and α_{RP} and hence it is not possible to determine. Therefore, a minimization procedure was adopted to maximize R^2, between the theoretical data for q_e predicted from the linearized form of Redlich-Peterson isotherm equation and the experimental data. Trial and error method was adopted to select constant, α_{RP} through optimization of R^2. Redlich-Peterson isotherm plot for the As(III) adsorption on all three adsorbents are presented in Fig. 9 and the isotherm parameters is given in Table 1. Redlich-Peterson constant, α_{RP} modifies Langmuir curve. The value of α_{RP} greater than unity shows the steeper slope in Langmuir isotherm equation. The higher R^2 values for Redlich-Peterson were obtained, which indicates that the experimental equilibrium data is more consistent with Redlich-Peterson isotherm equation. This was expected, because a degree of heterogeneity (α_{RP}) is included and this equation can be used successfully at high solute concentrations (Feng-Chin et al., 2010).

Table 1: Isotherms parameters for adsorption of As(III) on the adsorbents

Adsorbents	Freundlich			Langmuir					Temkin			Redlich-Peterson			
	K_f	1/n	R^2	q_m	b	R^2	R_L		K_T	b_t	R^2	K_{RP}	b_{RP}	α_{RP}	R^2
	$L.mg^{-1}$			$mg.g^{-1}$	$L.mg^{-1}$		Range		$L.mg^{-1}$	kJ.mole^{-1}		$mg.g^{-1}$	$L.mg^{-1}$		
BG	0.265	0.499	0.898	1.35	0.240	0.996	0.029	0.294	2.697	0.278	0.962	0.278	0.105	1.15	0.999
MB	0.310	0.121	0.921	1.25	0.326	0.999	0.021	0.235	4.834	0.230	0.984	0.407	0.326	1.00	0.999
GL	0.257	0.423	0.895	1.05	0.327	0.998	0.021	0.234	4.262	0.201	0.969	0.257	0.158	1.11	0.999

BG = bagasse, MB = mango bark and GL = guava leaf biomass

3.2.5 Comparison of isotherm models

Adsorption isotherms were analyzed using the postulates made by Freundlich, Langmuir, Temkin and Redlich–Peterson and ultimate capacity of adsorbents to adsorb As(III) were computed. Quasi-Gaussian energetic heterogeneity of the adsorption surface obtained from Freundlich isotherm indicates the better adsorption of As(III) on the surface of bagasse and least adsorption on mango bark. However, the value of Freundlich constant K_f shows that bagasse has maximum tendency to adsorb ions followed by mango bark and guava leaf biomass. Single layer adsorption of ions on guava leaf biomass and bagasse surface was reported by Freundlich isotherm. The parameter '1/n' measures adsorption intensity of As(III) on the adsorbents. Higher value of '1/n' on bagasse (0.499) in comparison to guava leaf biomass (0.432) and mango bark (0.121), indicates towards preferential sorption of As(III) on bagasse than on guava leaf biomass or mango bark. It also represented ability of the adsorbents to remove As(III) from solution even at high concentrations. Values of ultimate adsorption capacity K_f ($L.g^{-1}$) of the adsorbents were calculated from the linear regression equation (Fig. 6). The K_f value of mango bark (0.310 $L.g^{-1}$)

411 is more than that of bagasse (0.265 $L.g^{-1}$) and guava leaf biomass (0.257 $L.g^{-1}$), suggesting and
412 confirming that mango bark has greater adsorption tendency to adsorb arsenic than the other two
413 adsorbents. The lower value of coefficient of determination (R^2) for As(III) adsorption on surface
414 of guava leaf biomass (0.895) and bagasse (0.898) indicates the possibility of single layer
415 adsorption, however higher R^2 for mango bark (0.921) indicates towards multilayer adsorption of
416 arsenite species.
417 Separation factor observed for each adsorbent indicate favorable adsorption on adsorbent. Value
418 of R^2 (>0.900) calculated for each adsorbent is also indicate the applicability Langmuir
419 hypothesis i.e., monolayer adsorption and adsorption sites will be independent of the occupation
420 of neighboring sites with the accommodation of only one adsorbed atom on each adsorption site
421 in the form of complexes of reactive functional groups present on the surface of adsorbent.
422 Quantity of As(III) required to form a single monolayer on unit mass of adsorbent calculated
423 using Langmuir isotherm indicate that bagasse has higher adsorption capacity as 1.346 $mg.g^{-1}$ in
424 comparison to mango bark 1.249 $mg.g^{-1}$ and guava leaf biomass 1.052 $mg.g^{-1}$. Apparent energy
425 of sorption for adsorbent showed that adsorption on guava leaf biomass is more effective as
426 compare to mango bark and guava leaf biomass. Equilibrium binding constant ($L.mg^{-1}$)
427 calculated from Temkin isotherm showed that bagasse has least potential to adsorb As(III). Heat
428 of sorption was observed as bagasse for 0.278 $kJ.mole^{-1}$, mango bark for 0.230$kJ.mole^{-1}$ and
429 guava leaf biomass for 0.201 $kJ.mole^{-1}$. Relatively lower values in this study indicates a weak
430 interaction between sorbate and sorbent for ion-exchange mechanism. Introduction of
431 heterogeneity factor in Langmuir isotherm gave more appropriate isotherm to describe the
432 adsorption of As(III). Higher values of R^2 (>0.999) for Redlich-Peterson and Langmuir showed
433 that both isotherms are more applicable and appropriate in describing the experimental data and

confirm the monolayer adsorption of As(III) on the solid surface of the adsorbents. Uptake rates of As(III) on adsorbent surfaces was further studied using various models involving pseudo-first-order, pseudo-second-order, Elovich and intra-particle diffusion. Kinetic parameters were also investigated to comprehend the pattern of uptake.

3.3 Adsorption kinetics

Most of the sorption/ desorption processes of various solid phases are time-dependent. Knowledge of these kinetic processes are essential to understand the solute uptake rate and evidently this rate controls the residence time of adsorbate uptake at solid-solution interface (Mamy and Barriuso, 2006). The dynamic interactions of As(III) adsorption on the adsorbents of bagasse, mango bark and guava leaf biomass were analyzed to predict their fate with time using pseudo-first-order, pseudo-second-order, Elovitch and intra-particle diffusion kinetics. The conformity between experimental data and model predicted values were expressed by R^2.

3.3.1 Pseudo-first-order kinetic model

Pseudo-first-order equation or Lagergren's kinetic equation for the adsorption of adsorbate from aqueous solution is generally expressed by equation (12) and after integration and applying boundary conditions t = 0 to t = t and q = 0 to q = q, it is represented by equation (13).

$$\frac{dq}{dt} = k_1(q_e - q) \quad (12)$$

$$Ln(q_e - q) = Ln(q_e) - k_1 t \quad (13)$$

Where, q and q_e, is the amount of As(III) adsorbed per unit mass of adsorbent, ($mg.g^{-1}$) at time t and equilibrium respectively, k_1 is the pseudo-first-order rate constant, ($L.min^{-1}$) and t is the contact time (min). Pseudo-first-order kinetic model was chosen to estimate the As(III) adsorption rate constant from the experimental batch study.

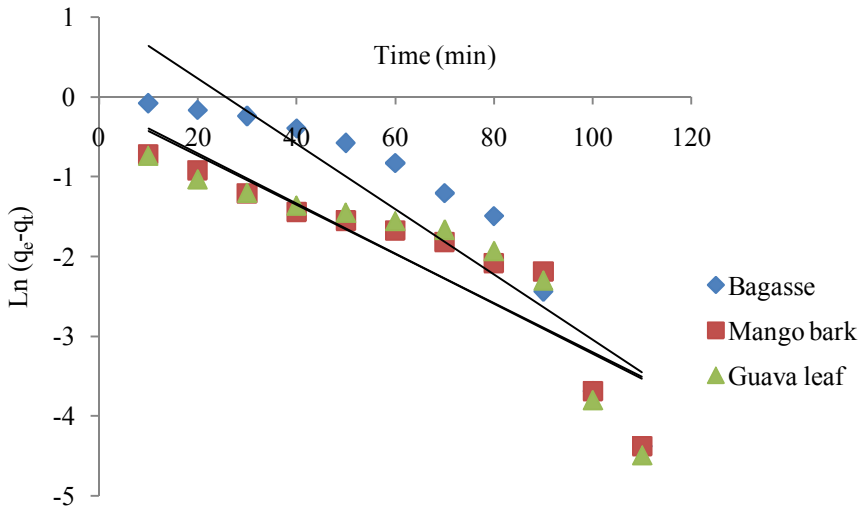

Figure 10: Pseudo-first-order plot for kinetic on As(III) adsorption

The plot of $Ln(q_e-q)$ vs t shown in Fig. 10 was used to find rate constant and is reported in Table 2. Almost same adsorption rate constant were observed for each adsorbent. Bagasse has slightly higher rate constant as 11.66×10^{-3} min^{-1} in comparison to 11.55×10^{-3} min^{-1} for guava leaf biomass and 11.50×10^{-3} min^{-1} for mango bark. Lower value of R^2 was observed for all the adsorbents which indicates that rate of adsorption of As(III) on adsorbent surface in not in proportion to $k_1(q_e-q)$ and does not represent true number of available sites for further adsorption on adsorbents surface. Possibility of As(III) present in aqueous solution to be adsorbed at saturated condition was found to be 6.983 $mg.g^{-1}$ (bagasse) in comparison to experimental value of 1.088 $mg.g^{-1}$ (Table 2), 5.062 $mg.g^{-1}$ (mango bark) against true experimental value of 1.050 $mg.g^{-1}$ and 5.212 $mg.g^{-1}$ (guava leaf biomass) against 0.922 $mg.g^{-1}$. It may be due to the fact that $Ln(q_e)$ is an adjustable parameter and often it is found to be not equal to the intercept of the plot $Ln(q_e-q)$ vs t (Kiskuet al., 2015; Tiwari et al., 2013). All these indicate that first-order-kinetic is inadequate to represent good account of the adsorption kinetics of As(III).

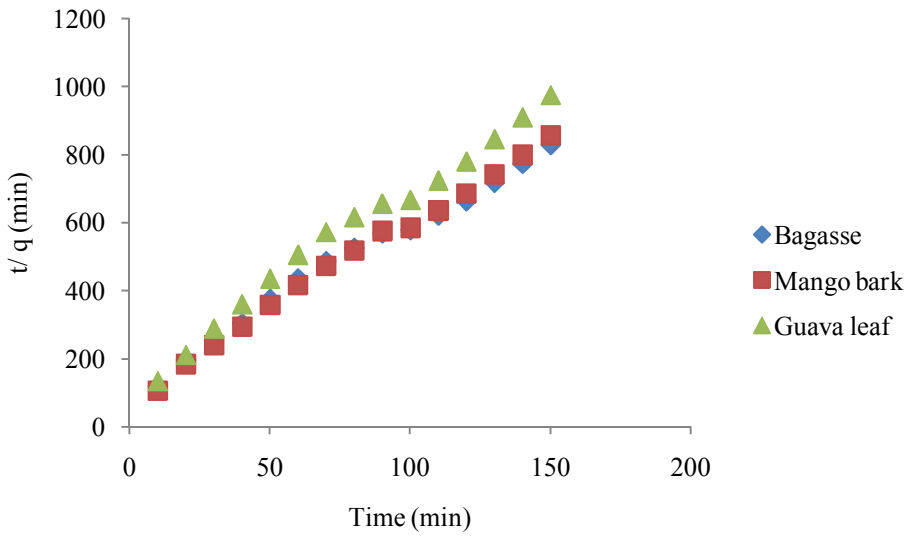

Figure 11: Pseudo-second-order plot (Type 1) for kinetic on As(III) adsorption

3.3.2 Pseudo-second-order kinetic model

Pseudo-second-order adsorption equation is expressed by equation (14). On further integrating and applying boundary conditions, t = 0 to t = t and q = 0 to q = q, it is linearized and presented in equation (16) and (17) as Type 1 kinetic and Type 2 kinetic by Markandeya et al. (2018). Pseudo-second-order rate constant, k_2 ($g.mg^{-1}.min^{-1}$)and ultimate adsorption capacity of adsorbent, q_e($mg.g^{-1}$)were obtained from the plot of t/q vs t (Type 1) (Fig. 11) and 1/q vs 1/t (Type 2) (Fig. 12), respectively and are reported in Table 2.

$$\frac{dq}{dt} = k_2(q_e - q)^2 \quad (14)$$

$$\frac{1}{q_e - q} = \frac{1}{q_e} + k_2 t \quad (15)$$

Type 1: $$\left(\frac{t}{q}\right) = \frac{1}{k_2\, q_e^2} + \frac{1}{q_e}(t) \quad (16)$$

Type 2: $$\left(\frac{1}{q}\right) = \frac{1}{q_e} + \left(\frac{1}{k_2\, q_e^2}\right)\frac{1}{t} \quad (17)$$

Markandeya et al. (2015) have defined another adsorption rate parameter, h ($mg.g^{-1}min^{-1}$) by equation (16) to study the initial adsorption rate as equation (18).

$$h = k_2 q_e^2 \quad (18)$$

Experimental observation presented in Figs. 10 and 13 indicated three stages of adsorption. Highest initial adsorption rate was observed for adsorption on mango bark for 0.011 $mg.g^{-1}.min^{-1}$ in comparison with bagasse (0.009 $mg.g^{-1}min^{-1}$) and guava leaf biomass (0879 $mg.g^{-1}min^{-1}$) for Type 1 kinetic. Similar trend for h was also reported for Type 2 kinetic and is presented in Table 2. It indicates that at beginning As(III) uptake on adsorbents will be more for mango bark followed by bagasse and guava leaf biomass. This As(III) uptake on adsorbent surface is from the diffusion of metal ion species on the boundary of adsorbent mainly due to their concentration gradient resulting with high uptake rate. However, adsorption will go on decreasing as concentration gradient decreases.

Table 2: Kinetic adsorption parameters for adsorption of As(III) on adsorbents

Adsorbents	$q_{e\,(exp)}$	Pseudo-first-order			Pseudo-second-order							
		k_1	R^2	$q_{e\,(cal)}$	Type 1				Type 2			
					k_2	h	R^2	$q_{e\,(cal)}$	k_2	h	R^2	$q_{e\,(cal)}$
	$mg.g^{-1}$	min^{-1}		$mg.g^{-1}$	$g.mg^{-1}min^{-1}$	$mg.g^{-1}.min^{-1}$		$mg.g^{-1}$	$g.mg^{-1}min^{-1}$	$mg.g^{-1}.min^{-1}$		$mg.g^{-1}$
BG	1.088	11.66×10^{-3}	0.771	6.983	53.20×10^{-4}	0.009	0.987	1.267	11.41×10^{-3}	0.014	0.923	1.099
MB	1.050	11.55×10^{-3}	0.801	5.062	80.32×10^{-4}	0.011	0.994	1.117	15.69×10^{-3}	0.018	0.916	1.060
GL	0.922	11.50×10^{-3}	0.800	5.212	69.63×10^{-4}	0.008	0.987	1.060	15.11×10^{-3}	0.013	0.917	0.928

Second and third stage of adsorption is due to formation of inner-sphere mono-dentate and bi-dentate surface complexes that depends upon the composition and texture of the adsorbent surface. These inner sphere complexes are covalent linkage between As(III) and reactive surface functional groups present in the adsorbents (Carabante et al., 2009).

503 Pseudo-second-order adsorption rate, k_2 was more for mango bark (80.32×10^{-5} $g.mg^{-1}min^{-1}$)
504 followed by guava leaf biomass (69.63×10^{-5} $g.mg^{-1}min^{-1}$) and bagasse (53.21×10^{-5} $g.mg^{-1}min^{-1}$)
505) in comparatively slower rate. Adsorption capacity predicted by type 2 kinetic has more closure
506 value to its experiment value as compared to Type 1. It indicates that adsorption sites for As(III)
507 uptake on each adsorbent can be represented by $k_2(q_e-q)^2$. This capacity for metal complexation
508 depends upon the affinity and specificity including physico-chemical nature of functional groups
509 present in adsorbents (Sud et al., 2008). Higher value of R^2 was observed for mango bark (0.994)
510 and same value for bagasse and guava leaf biomass (0.987) as reported by Type 1 kinetic. Type 2
511 kinetic also reported a very little difference in R^2 values for each adsorbent. This higher value of
512 R^2 (>0.90) makes the applicability of second order kinetic for adsorption of As(III) on each
513 adsorbent.

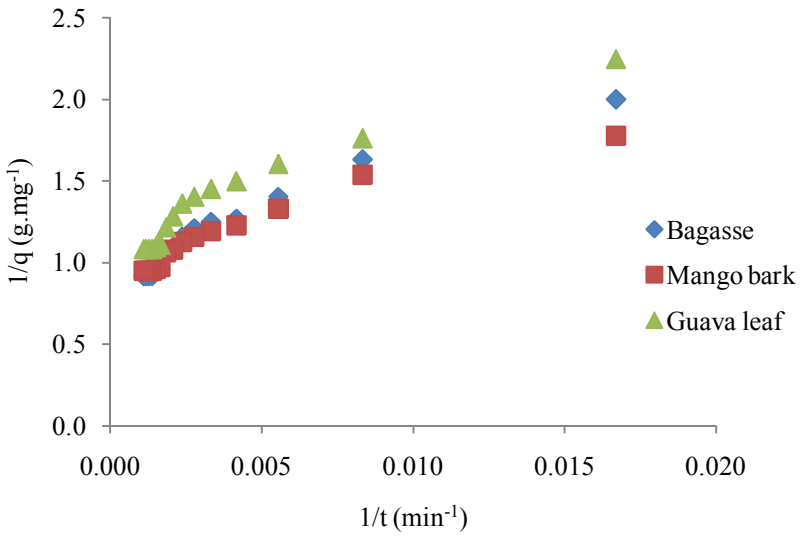

514
515 Figure 12: Pseudo-second-order plot (Type 2) for kinetic on As(III) adsorption

516 **3.3.3 Elovich kinetic model**

517 Elovich kinetic equation is generally expressed by equation (19) as given below.

518 $$\frac{dq}{dt} = \alpha e^{(-\beta q)} \quad (19)$$

519 Where α is the initial adsorption rate ($mg.g^{-1}.min^{-1}$) and β is desorption constant ($g.mg^{-1}$) during
520 any experiment. Simplification of equation (19) proposed by Chien and Clayton (1980) and by
521 applying the boundary conditions t = 0 to t = t and q = 0 to q = q, it is represented by equation
522 (20).

523 $$q = \frac{1}{\beta} Ln(\alpha\beta) + \frac{1}{\beta} Ln(t) \quad (20)$$

524 Desorption constant and initial adsorption rate were calculated from the slope and intercept of
525 plot of q vs Ln(t) (Fig. 13) and reported in Table 3. Higher initial rate for mango bark (0.049
526 $mg.g^{-1}.min^{-1}$) was observed in comparison with guava leaf biomass (0.028 $mg.g^{-1}.min^{-1}$) and
527 bagasse (0.026 $mg.g^{-1}.min^{-1}$). It shows that As(III) have higher affinity to form inner-sphere
528 mono-dentate surface complexes. Desorption constant was reported maximum for guava leaf
529 biomass (5.257 $g.mg^{-1}$) followed by mango bark (5.086 $g.mg^{-1}$) and bagasse (4.228 $g.mg^{-1}$),
530 respectively. It shows that bagasse has strong covalent linkage between As(III) and reactive
531 functional group present in the adsorbents in comparison to mango bark and guava leaf biomass.
532 Higher values of R^2 (>0.90) were observed for all adsorbents, indicating applicability of the
533 model.

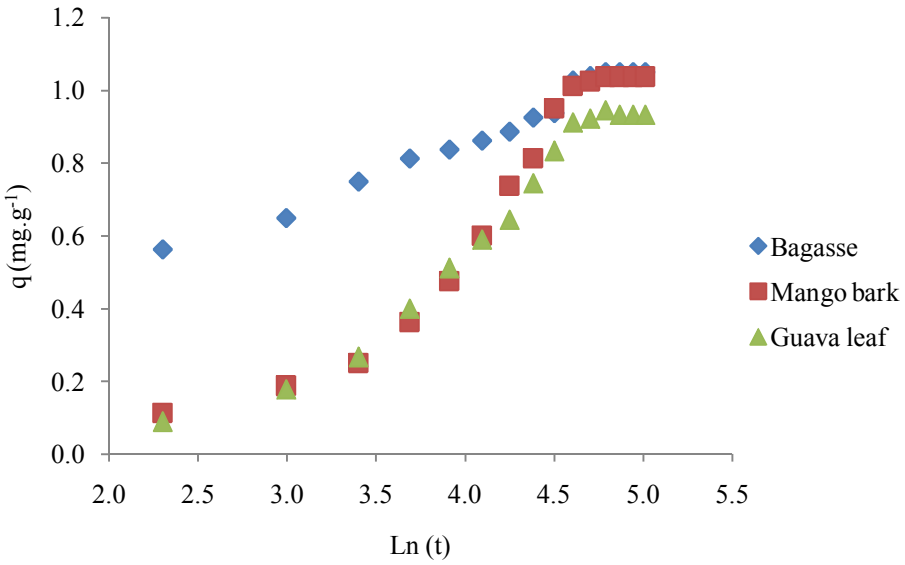

Figure 13: Elovich plot for the kinetic of As(III) adsorption

3.3.4 Intra-particle diffusion model

Intra-particle model defined by Weber and Morris (1963) followed by linearization is represented in equation (21) and (22) respectively.

$$R = k_{id}(t)^{a} \quad (21)$$

$$Ln(R) = Ln(k_{id}) + aLn(t) \quad (22)$$

Where, R is the percentage As(III) adsorbed, t is the contact time (min), a is diffusion factor for the adsorption and depicts the adsorption mechanism and k_{id} is the intra-particle diffusion rate constant (min^{-1}) i.e. percentage As(III) adsorbed per unit time. Diffusion factor and rate constant was determined from the slope and intercept of the plot of Ln(R) vs Ln(t) (Fig. 14) and is reported in Table 3.

Table 3: Kinetic adsorption parameters for adsorption of As(III) on adsorbents

Adsorbent	Elovich model			Intra-particle diffusion model		
	A $mg.g^{-1}.min$	β $g.mg^{-1}$	R^2	k_{id} min^{-1}	a $\%.min^{-1}$	R^2
BG	0.026	4.228	0.966	11.87	0.298	0.986
MB	0.049	5.086	0.977	16.77	0.242	0.986
GL	0.028	5.257	0.957	13.16	0.275	0.978

BG = bagasse, MB = mango bark and GL = guava leaf biomass

Data presented in Table 2, 5.062 $mg.g^{-1}$ shows maximum diffusion rate for mango bark followed by guava leaf biomass and bagasse. But diffusion factor, 'a' is lowest for mango bark in comparison to guava leaf biomass and bagasse. Higher values of k_{id} demonstrate an enrichment in the rate of adsorption, whereas large 'a' values illustrate a better adsorption mechanism, which is related to an improved bonding between adsorbate and adsorbent species (Bhargava and Bhatt, 1985).

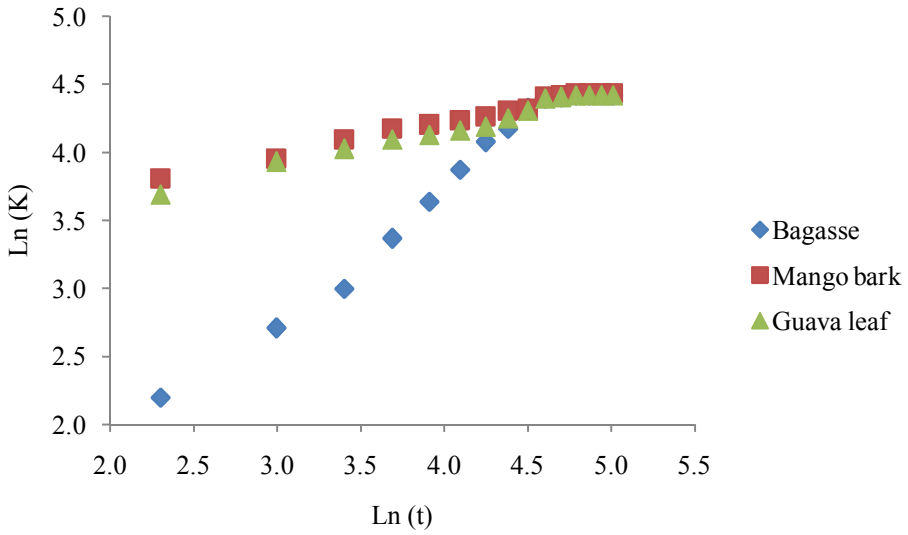

Figure 14: Intra-particle plot for the kinetic of As(III) adsorption

3.3.5 Comparison of kinetic models

Kinetic studies for the adsorption of As(III) on adsorbents of bagasse, mango bark and guava leaf biomass were conducted using pseudo-first-order, pseudo-second-order, Elovich and intra-

560 particle diffusion models which are shown in Figs. 10 to 14 and kinetic parameters are reported
561 in Tables 2 and 3. Higher value of R^2 and perfect straight lines were obtained for pseudo-second-
562 order kinetic plot of (t/q) vs (t) for adsorption of As(III) on all adsorbents, indicating that first
563 order adsorption reaction is not adequate and pseudo-second-order kinetic model can be
564 approximated a good account of adsorption kinetics. Initial rate constant obtained from all
565 kinetic models shows that molecules of mango bark has higher tendency to form mono and bi-
566 dentate complexes giving more affinity between As(III) and adsorbent surface. However, results
567 of intra-particle diffusion and Elovich kinetic model indicates that mango bark has lower
568 bonding linkage of As(III) on adsorbent surface after 2-3 hr of adsorption, indicating
569 comparatively poor adsorption capability. Results of these models also indicate that adsorbent of
570 bagasse has more adsorption ability followed by guava leaf biomass and mango bark.

571 **4. Conclusions**

572 Extensive laboratory investigations were conducted to evaluate the adsorptive capability of low-
573 cost adsorbent prepared from materials of bagasse, mango bark and guava leaf biomass for
574 adsorption of As(III) and results indicated that these adsorbents have the adsorptive capacity to
575 treat arsenic contaminated water. Kinetic parameters calculated from Elovich and intra-particle
576 model indicate that bagasse has better adsorption mechanism followed by other adsorbent of
577 guava leaf biomass and mango bark. Contact time, adsorbent dosage and pH were observed to be
578 amongst the most effective controlling parameters for As(III) adsorption. Adsorbents of bagasse,
579 mango bark and guava leaf biomass has maximum removal of As(III) at 7.5, 6.5 and 6.0,
580 respectively. Pseudo-second-order kinetic for adsorption of As(III) was followed in three stages.
581 First stage of adsorption was rapid diffusion of As(III) from aqueous solution to boundary of
582 adsorbent pores followed by arrangement of adsorption sites through the formation of inner

583 spherical mono-dentate complexes and finally, formation of bi-dentate complexes within very
584 short duration. Monolayer adsorption of As(III) on adsorbents was confirmed by Freundlich,
585 Langmuir and Redlich–Peterson model. Adsorption capacity on surface of bagasse obtained from
586 Langmuir isotherms was highest for as 1.35 $mg.g^{-1}$ in comparison to mango bark (1.25 $mg.g^{-1}$)
587 and guava leaf biomass (1.05 $mg.g^{-1}$).

588 **Acknowledgement**

589 Authors are gratitude to the Director, IIT-BHU, Varanasi for providing necessary facilities to this
590 research. There is no conflict of interest in the present study.

591 **References**

592 APHA, Standard method for the examination of water and wastewater, 22nd Eds., American
593 Water Works Association and Water Pollution Control Federation, Washington, 2012.

594 Babu, B. V., Gupta, S., Adsorption of Cr(VI) using activated neem leaves: kinetic study.
595 Adsorption, 2008, 13, 85–92. doi:10.1007/s10450-007-9057-x

596 Bhargava, D. S., Bhatt, D. J., Model for moving media reactor performance. J. Environ. Eng.,
597 1985, 111(5), 618–633. doi:10.1061

598 Carabante, I., Grahn, M., Holmgren, A., Kumpiene, A., Hedlund, J., Adsorption of As(V) on
599 oxide nanoparticle films studied by in situ ATR-FTIR spectroscopy. Colloids and Surfaces A:
600 Physicochem. Eng. Aspects, 2009, 346, 106–113.doi:10.1016/j.colsurfa.2009.05.032

601 Chien,S. H., Clayton,W. R., Application of Elovich equation to the kinetics of phosphate release
602 and sorption in soils. Soil Sci. Soc. America J., 1980, 44(2), 265–268.
603 doi:10.2136/sssaj1980.03615995004400020013x

Choong, Y. S. T., Chuah, G. T., Robia, H. Y., Koay, L. F. G., Azni, I., Arsenic toxicity, health hazards and removal techniques from water: an overview. Desalination, 2007, 217, 39–166. doi:10.1016/j.desal.2007.01.015

Feng-Chin, W., Bing-Lan, L., Keng-Tung, W., Ru-Ling, T., A new linear form analysis of Redlich–Peterson isotherm equation for the adsorptions of dyes. Chem. Eng. J., 2010, 162, 21–27. doi:10.1016/j.cej.2010.03.006

Freundlich, H. Z., Over the Adsorption in solution. J. Physical Chem., 1906, 57, 385–470.

Jain, C. K., Singh, R. D., Technological options for the removal of arsenic with special reference to South East Asia: Review. J. Environ. Manag., 2012, 107, 1–18. doi:10.1016/j.jenvman.2012.04.016

Jeong, Y., Maohong, F., Leeuwen, J. V., Belczyk, J. F., Effect of competing solutes on arsenic(V) adsorption using iron and aluminum oxides. J. Environ. Scie., 2007, 19, 910–919. doi:10.1016/S1001-0742(07)60151-x

Katsoyiannis, I. A., Zouboulis, A. I., Application of biological processes for the removal of arsenic from ground waters. Water Res., 2004, 38, 17–26. doi:10.1016/j.watres.2003.09.011

Kim, J., Benjamin, M. M., Modeling a novel ion exchange process for arsenic and nitrate removal. Water Res., 2004, 38(8), 2053–2062. doi:10.1016/j

Kisku, G. C., Markandeya, Shukla, S. P., Singh, D. S., Murthy, R. C., Characterization and adsorptive capacity of coal fly ash from aqueous solutions of disperse blue and disperse orange dyes. Environ. Earth Sci., 2015, 74(2), 1125-1135.

Kumar, K. V., Linear and non-linear regression analysis for the sorption kinetics of methylene blue onto activated carbon. J. Hazard. Mater., 2006, B137, 1538-1544. doi:10.1016/j.jhazmat.2006.04.036

627 Langmuir, I., The adsorption of gases on plane surfaces of glass, mica, and platinum. J.
628 American Chem. Soc., 1916, 40, 1361–1403. doi:10.1021/ja02242a004
629 Leupin, O. X., Hug, S. J., Oxidation and removal of Arsenic(III) from aerated groundwater by
630 filtration through sand and zero-valent iron. Water Resources, 2005, 39(9), 1729–1740.
631 doi:10.1016/j.watres.2005.02.01
632 Mamy, L., Barriuso, E., Desorption and time-dependent sorption of herbicides in soils. European
633 J. Soil Sci., 2006, 58, 174-187. doi:10.1111/j.1365-2389.2006.00822.x
634 Mandal, B. K., Suzuki, K. T., Arsenic round the world: A review. Talanta, 2002, 58, 201–235.
635 doi:10.1177/0960327107084539
636 Markandeya, Dhiman, N., Shukla, S. P., Kisku, G. C., Statistical optimization of process
637 parameters for removal of dyes from wastewater on chitosan cenospheres nanocomposite using
638 response surface methodology. J. Cleaner Prod., 2017a, 149, 597-606.
639 Markandeya, Dhiman, N., Shukla, S. P., Mohan, D., Kisku, G. C., Patnaik, S., Comprehensive
640 remediation study of disperse dyes containing wastewater by using environmental benign, low
641 cost cenospheresnanosyntactic foam. J. Cleaner Prod., 2018, 182, 206-216.
642 Markandeya, Shukla, S. P., Dhiman, N., Characterization and adsorption of disperse dyes from
643 wastewater onto cenospheres activated carbon composites. Environ. Earth Sci. 2017b, 76, 702-
644 714.
645 Markandeya, Shukla, S. P., Dhiman, N., Mohan, D., Kisku, G. C., Roy, S., An efficient removal
646 of disperse dye from wastewater using zeolite synthesized from cenospheres. J. Hazardous,
647 Toxic, and Radio. Waste, 2017c, 21(4), 04017017.
648 Markandeya, Shukla, S. P., Kisku, G. C., Linear and non-linear kinetic modeling for the
649 adsorption of disperse dye in a batch process.Res. J. Environ. Toxico., 2015, 9(6), 320-331.

650 Markandeya, Shukla, S. P., Mohan, D., Toxicity of disperse dyes and its removal from
651 wastewater using various adsorbents: a review. Res. J. Environ. Toxico., 2017d, 9, 01-18.
652 Markandeya, Singh, A., Shukla, S. P., Mohan, D., Singh, N. B., Bhargava, D. S., Shukla, R.,
653 Pandey, G., Yadav, V. P., Kisku, G. C., Adsorptive capacity of sawdust for the adsorption of MB
654 dye and designing of two-stage batch adsorber. Cogent Environ. Sci., 2015, 1(1), 1075856.
655 Mohan, D., Charles, P., Arsenic removal from water/wastewater using adsorbents – A critical
656 review. J. Hazard. Mater., 2007, 142(1–2), 1–53. doi:10.1016/j.jhazmat.2007.01.006
657 Mohan, D., Pittman, C. U. Bricka, M., Smith, F., Yancey, B., Mohammad, J., Steele, P. H.,
658 Alexandre-Franco, M. F., Serrano, V. G., Gong, H., Sorption of arsenic, cadmium, and lead by
659 chars produced from fast pyrolysis of wood and bark during bio-oil production. J. Colloid and
660 Inter. Sci., 2007, 310(1), 57–73. doi:10.1016/j.jcis.2007.01.020
661 Montagnaro, F., Santoro, L., Reuse of coal combustion ashes as dyes and heavy metal
662 adsorbents: effect of sieving and demineralization on waste properties and adsorption capacity.
663 Chem. Eng. J., 2009, 150, 174–180. doi:10.1016/j.cej.2008.12.022
664 Natale, F. D., Erto, A., Lancia, A., Musmarra, D., Experimental and modeling analysis of As(V)
665 ions adsorption on granular activated carbon. Water Res., 2008, 42, 2007–2016.
666 doi:10.1016/j.watres.2007.12.008
667 Peggy, A. O., Chemistry and Mineralogy of Arsenic. Elements, 2006, 2(2), 77–83.
668 doi:10.2113/gselements.2.2.77
669 Qaiser, S., Saleemi, A. R., Ahmad, M. M., Heavy metal uptake by agro based waste materials.
670 Environ. Biotech., 2007, 10, 409–416. doi:10.2225/vol10-issue3-fulltext-12
671 Rahman, M. M., Mukherjee, D., Sengupta, M. K., Chowdhury, U. K., Lodh, D., Chanda, C. R.,
672 Roy, S., Selim, M. D., Quamruzzaman, Q., Milton, A. H., Shahidullah, S. M., Rahman, M. T.,

673 Chakraborti, D., Effectiveness and reliability of arsenic field testing kits: are the million dollar
674 screening projects effective or not. Environ. Sci. Tech., 2002, 36(24), 5385–5394.
675 doi:10.1021/es020591o
676 Redlich, O., Peterson, D. L., A useful adsorption isotherm. J. Physical Chem., 1959, 63, 1024–
677 1029. doi:10.1021/j150576a611
678 Salman, M., Athar, M., Shafique, M., Din, M. I., Rehman, R., Akram, A., Ali, S. Z., Adsorption
679 modeling of alizarin yellow on untreated and treated charcoal. Turkish J. Eng. Environ. Sci.,
680 2011, 35, 209–216. doi:10.3906/muh-1009-32
681 Shevade, S., Ford, R., Use of synthetic zeolites for arsenate removal from pollutant water. Water
682 Res., 2004, 38, 3197–3204. doi:10.1016/j.watres.2004.04.026
683 Shipley, H. J., Yean, S., Kan, A. T., Tomson, M. B., Adsorption of arsenic to magnetite
684 nanoparticles: Effect of particle concentration, pH, ionic strength, and temperature. Environ.
685 Toxic. Chem., 2009, 28(3), 509–515. doi:10.1897/08-155.1
686 Shukla, N. K., Markandeya, Shukla, V. K., Arsenic and physico-chemical calamity in the ground
687 water samples of Ballia district, Uttar Pradesh, India. Iranica J. Energy and Environ., 2015, 6(4),
688 328-333.
689 Shukla, S. P., Singh, A., Dwivedi, L., Sharma, K. J., Bhargava, D. S., Shukla, R., Singh, N. B.,
690 Yadav, V. P., Markandeya, Minimization of contact time for two-stage batch adsorber design
691 using second-order kinetic model for adsorption of methylene blue (MB) on used tea leaves.
692 Inter. J. Sci. Innov. Res., 2014, 2(1), 58–66.
693 Shukla, S. P., Sonam, Markandeya, Mohan, D., Pandey, G., Removal of fluoride from aqueous
694 solution using Psidium guajava leaves. Desal. Water Treat., 2017, 62, 418-425.

695 Singh, T. S., Pant, K. K., Equilibrium, kinetics and thermodynamic studies for adsorption of
696 As(III) on activated alumina. Sep. Purification Tech., 2004, 36, 139–147. doi:10.1016/S1383-
697 5866(03)00209-0
698 Sud, D., Mahajan, G., Kaur, M. P., Agricultural waste material as potential adsorbent for
699 sequestering heavy metal ions from aqueous solutions: a review. Biores. Tech., 2008, 99, 6017–
700 6027. doi:10.1016/j.biortech.2007.11.064
701 Tamas, M. J., Sharma, S. K., Ibstedt, S., Jacobson, T., Christen, P., Heavy metals and metalloids
702 as a Cause for protein misfolding and aggregation. Biomolecules, 2014, 4, 252-267.
703 doi:10.3390/biom4010252
704 Temkin, M. J. Pyzhev, V., Kinetics of ammonia synthesis on promoted iron catalysts. Acta
705 Physiochimica URRS, 1940, 12, 217–222.
706 Tiwari, M., Shukla, S. P., Bhargava, D. S., Kisku, G. C., Color removal potential of coal fly ash-
707 a low cost adsorbent from aqueous solutions of disperse dyes used in textile mill through batch
708 technique. Our Earth, 2013, 10(4), 5–8.
709 Tiwari, M., Shukla, S. P., Mohan, D., Bhargava, D. S., Kisku, G. C., Modified cenospheres as an
710 adsorbent for the removal of disperse dyes. Adv. Environ. Chem., 2015, 2015, 1-8.
711 USEPA, Arsenic occurrence in public drinking water supplies. U. S. Environmental Protection
712 Agency, Washington, D. C., 2007, EPA-815-R-00-023, 1–156.
713 USEPA, Federal Register, U. S. Environmental Protection Agency, Washington, D. C., 2001,
714 66(14), 6976–7066.
715 Vaishya, R. C., Gupta, S. K., Modeling Arsenic(V) removal from water by sulfate modified iron-
716 oxide coated sand (SMIOCS). J. Chem. Tech. Biotech., 2002, 78, 73–80.

717 Wang, J., Chen, C., Biosorbents for heavy metals removal and their future: Review. Biotech.
718 Advances, 2009, 27, 195–226. doi:10.1016/j.biotechadv.2008.11.002
719 Wang, S., Boyjoo, Y., Choueib, A., Zhu, Z. H. , Removal of dyes from aqueous solution using
720 fly ash and red mud. Water Res., 2005, 39, 129–138. doi:10.1016/j.watres.2004.09.011
721 Weber, W. J., Matcalf, R. L., Pitts, J. N., Adsorption in physicochemical process for water
722 quality control. Wiley Intersci., New York, 1972, 199–259.
723 Weber, W. J., Morris, J. C., Kinetics of adsorption on carbon from solution. J. Sanitary Eng.
724 Div., 1963, 89, 31–60.
725 Weng, Y. H., Chaung-Hsieh, L. H., Lee, H. H., Li, K. C., Huang, C. P., Removal of arsenic and
726 humic substances (HSs) by electro-ultrafiltration (EUF). J. Hazard. Materials, 2005, 122(1–2),
727 171–176. doi:10.1016/j.jhazmat.2005.04.001
728 WHO, Arsenic compounds, environmental health criteria 224. 2nd Eds., World Health
729 Organization, Geneva, 2001.
730 Wickramasinghe, S. R., Han, B., Zimbron, J., Shen, Z., Karim, M. N., Arsenic removal by
731 coagulation and filtration: comparison of groundwater from the United States and Bangladesh.
732 Desalination, 2004, 169(3), 231–244. doi:10.1016/S0011-9164(04)00530-2